

## Event-by-Event Fluctuations in Particle Multiplicities and Transverse Energy Produced in 158-A GeV Pb+Pb collisions

M.M. Aggarwal,<sup>4</sup> Z. Ahammed,<sup>2</sup> A.L.S. Angelis,<sup>7</sup> V. Antonenko,<sup>13</sup> V. Arefiev,<sup>6</sup> V. Astakhov,<sup>6</sup> V. Avdeitchikov,<sup>6</sup> T.C. Awes,<sup>16</sup> P.V.K.S. Baba,<sup>10</sup> S.K. Badyal,<sup>10</sup> S. Bathe,<sup>14</sup> B. Batiounia,<sup>6</sup> T. Bernier,<sup>15</sup> K.B. Bhalla,<sup>9</sup> V.S. Bhatia,<sup>4</sup> C. Blume,<sup>14</sup> D. Bucher,<sup>14</sup> H. Büsching,<sup>14</sup> L. Carlén,<sup>12</sup> S. Chattopadhyay,<sup>2</sup> M.P. Decowski,<sup>3</sup> H. Delagrange,<sup>15</sup> P. Donni,<sup>7</sup> M.R. Dutta Majumdar,<sup>2</sup> K. El Chenawi,<sup>12</sup> A.K. Dubey,<sup>1</sup> K. Enosawa,<sup>18</sup> S. Fokin,<sup>13</sup> V. Frolov,<sup>6</sup> M.S. Ganti,<sup>2</sup> S. Garpman,<sup>12</sup> O. Gavrishchuk,<sup>6</sup> F.J.M. Geurts,<sup>19</sup> T.K. Ghosh,<sup>8</sup> R. Glasow,<sup>14</sup> B. Guskov,<sup>6</sup> H. Å.Gustafsson,<sup>12</sup> H. H.Gutbrod,<sup>5</sup> I. Hrivnacova,<sup>17</sup> M. Ippolitov,<sup>13</sup> H. Kalechofsky,<sup>7</sup> K. Karadjev,<sup>13</sup> K. Karpio,<sup>20</sup> B. W. Kolb,<sup>5</sup> I. Kosarev,<sup>6</sup> I. Koutcheryaev,<sup>13</sup> A. Kugler,<sup>17</sup> P. Kulinich,<sup>3</sup> M. Kurata,<sup>18</sup> A. Lebedev,<sup>13</sup> H. Löhner,<sup>8</sup> L. Luquin,<sup>15</sup> D.P. Mahapatra,<sup>1</sup> V. Manko,<sup>13</sup> M. Martin,<sup>7</sup> G. Martínez,<sup>15</sup> A. Maximov,<sup>6</sup> Y. Miake,<sup>18</sup> G.C. Mishra,<sup>1</sup> B. Mohanty,<sup>1</sup> M.-J. Mora,<sup>15</sup> D. Morrison,<sup>11</sup> T. Mukhanova,<sup>13</sup> D. S. Mukhopadhyay,<sup>2</sup> H. Naef,<sup>7</sup> B. K. Nandi,<sup>1</sup> S. K. Nayak,<sup>10</sup> T. K. Nayak,<sup>2</sup> A. Nianine,<sup>13</sup> V. Nikitine,<sup>6</sup> S. Nikolaev,<sup>6</sup> P. Nilsson,<sup>12</sup> S. Nishimura,<sup>18</sup> P. Nomokonov,<sup>6</sup> J. Nystrand,<sup>12</sup> A. Oskarsson,<sup>12</sup> I. Otterlund,<sup>12</sup> T. Peitzmann,<sup>14</sup> D. Peressounko,<sup>13</sup> V. Petracek,<sup>17</sup> S.C. Phatak,<sup>1</sup> W. Pinganaud,<sup>15</sup> F. Plasil,<sup>16</sup> M.L. Purschke,<sup>5</sup> J. Rak,<sup>17</sup> R. Raniwala,<sup>9</sup> S. Raniwala,<sup>9</sup> N.K. Rao,<sup>10</sup> F. Retiere,<sup>15</sup> K. Reygers,<sup>14</sup> G. Roland,<sup>3</sup> L. Rossetet,<sup>7</sup> I. Roufanov,<sup>6</sup> C. Roy,<sup>15</sup> J.M. Rubio,<sup>7</sup> S.S. Sambyal,<sup>10</sup> R. Santo,<sup>14</sup> S. Sato,<sup>18</sup> H. Schlagheck,<sup>14</sup> H.-R. Schmidt,<sup>5</sup> Y. Schutz,<sup>15</sup> G. Shabratova,<sup>6</sup> T.H. Shah,<sup>10</sup> I. Sibiriak,<sup>13</sup> T. Siemiarczuk,<sup>20</sup> D. Silvermyr,<sup>12</sup> B.C. Sinha,<sup>2</sup> N. Slavine,<sup>6</sup> K. Söderström,<sup>12</sup> G. Sood,<sup>4</sup> S.P. Sørensen,<sup>11</sup> P. Stankus,<sup>16</sup> G. Stefanek,<sup>20</sup> P. Steinberg,<sup>3</sup> E. Stenlund,<sup>12</sup> M. Sumbera,<sup>17</sup> T. Svensson,<sup>12</sup> A. Tsvetkov,<sup>13</sup> L. Tykarski,<sup>20</sup> E.C.v.d. Pijll,<sup>19</sup> N.v. Eijndhoven,<sup>19</sup> G.J.v. Nieuwenhuizen,<sup>3</sup> A. Vinogradov,<sup>13</sup> Y.P. Viyogi,<sup>2</sup> A. Vodopianov,<sup>6</sup> S. Vörös,<sup>7</sup> B. Wystouch,<sup>3</sup> G.R. Young<sup>16</sup>

(WA98 Collaboration)

<sup>1</sup> Institute of Physics, Bhubaneswar 751005, India

<sup>2</sup> Variable Energy Cyclotron Centre, Calcutta 700064, India

<sup>3</sup> MIT Cambridge, MA 02139

<sup>4</sup> University of Panjab, Chandigarh 160014, India

<sup>5</sup> Gesellschaft für Schwerionenforschung (GSI), D-64220 Darmstadt, Germany

<sup>6</sup> Joint Institute for Nuclear Research, RU-141980 Dubna, Russia

<sup>7</sup> University of Geneva, CH-1211 Geneva 4, Switzerland

<sup>8</sup> KVI, University of Groningen, NL-9747 AA Groningen, The Netherlands

<sup>9</sup> University of Rajasthan, Jaipur 302004, Rajasthan, India

<sup>10</sup> University of Jammu, Jammu 180001, India

<sup>11</sup> University of Tennessee, Knoxville, Tennessee 37966, USA

<sup>12</sup> University of Lund, SE-221 00 Lund, Sweden

<sup>13</sup> RRC "Kurchatov Institute", RU-123182 Moscow

<sup>14</sup> University of Münster, D-48149 Münster, Germany

<sup>15</sup> SUBATECH, Ecole des Mines, Nantes, France

<sup>16</sup> Oak Ridge National Laboratory, Oak Ridge, Tennessee 37831-6372, USA

<sup>17</sup> Nuclear Physics Institute, CZ-250 68 Rez, Czech Rep.

<sup>18</sup> University of Tsukuba, Ibaraki 305, Japan

<sup>19</sup> Universiteit Utrecht/NIKHEF, NL-3508 TA Utrecht, The Netherlands

<sup>20</sup> Institute for Nuclear Studies, 00-681 Warsaw, Poland

(October 29, 2018)

Event-by-event fluctuations in the multiplicities of charged particles and photons, and the total transverse energy in 158-A GeV Pb+Pb collisions are studied for a wide range of centralities. For narrow centrality bins the multiplicity and transverse energy distributions are found to be near perfect Gaussians. The effect of detector acceptance on the multiplicity fluctuations has been studied and demonstrated to follow statistical considerations. The centrality dependence of the charged particle multiplicity fluctuations in the measured data has been found to agree reasonably well with those obtained from a participant model. However, for photons the multiplicity fluctuations have been found to be lower compared to those obtained from a participant model. The multiplicity and transverse energy fluctuations have also been compared to those obtained from the VENUS event generator.

## I. INTRODUCTION

Fluctuations in physical observables in heavy ion collisions have been a topic of interest for some years as they may provide important signals regarding the formation of Quark-Gluon Plasma (QGP) and help to address the question of thermalization [1]. With the large number of particles produced in heavy ion collisions at SPS and RHIC energies [2,3], it has now become feasible to study fluctuations on an event-by-event basis. Recently, several new methods have been proposed for the study of event-by-event fluctuations in various global observables to probe the nature of the QCD phase transition [4–7]. In a thermodynamical picture of a strongly interacting system formed in the collision, the fluctuations in particle multiplicities, mean transverse momenta ( $\langle p_T \rangle$ ), and other global observables, are related to the fundamental properties of the system, such as the specific heat, chemical potential, and matter compressibility. These, in turn, lead towards understanding the critical fluctuations at the QCD phase boundary. The existence of a tri-critical point at the QCD phase transition [4], which has lately been a topic of intense discussion, has been predicted to be associated with large event-by-event fluctuations in the above observables.

In a first order phase transition scenario, it is believed that supercooling might lead to density fluctuations resulting in droplet formation and hot spots [8]. These might lead to rapidity fluctuations in the form of spikes and gaps in the rapidity distribution. The study of event-by-event fluctuations in the number of photons to charged particles has also been proposed as a means to search for production of Disoriented Chiral Condensates (DCC) [9,10].

In nucleus - nucleus collisions the transverse energy,  $E_T$ , is an extensive global variable [11–13] which provides a direct measure of the violence of an interaction.  $E_T$  is produced by redirection of the longitudinal energy into transverse motion through interactions in which the interacting particles undergo multiple scatterings and approach thermalization.  $E_T$  is also an indicator of the energy density achieved in the collision. Since the energy density is directly related to the QGP phase transition, it is extremely important to study  $E_T$  and fluctuations in  $E_T$ . Moreover it is interesting to compare the fluctuations of  $E_T$  to those observed in the particle multiplicities.

Much theoretical interest has been directed toward the subject of event-by-event fluctuations, motivated by the near perfect Gaussian distributions of  $\langle p_T \rangle$  and particle ratios [14] measured at the SPS. For these Gaussian distributions, the variance or the width of the distribu-

tions contain information about the reaction mechanism as well as the nuclear geometry [4,15–17].

The relative fluctuation ( $\omega_X$ ) in an observable  $X$  can be expressed as:

$$\omega_X = \frac{\sigma_X^2}{\langle X \rangle}, \quad (1)$$

where  $\sigma_X^2$  is the variance of the distribution and  $\langle X \rangle$  denotes the mean value.

The value of  $\omega_X$  which can be extracted from experimental data has contributions which originate both from trivial statistical effects as well as dynamical sources. To extract the dynamical part associated with new physics from the observed fluctuations, one has to understand the contributions from statistical and other known sources. Examples of known sources of fluctuations contributing to the observed experimental value of  $\omega_X$  include finite particle multiplicity, effect of limited acceptance of the detectors, impact parameter fluctuations, fluctuations in the number of primary collisions, effects of re-scattering of secondaries, resonance decays, and Bose-Einstein correlations. These sources of fluctuations, along with estimates of the  $\omega_X$  contributions for each have been discussed by Stephanov et al. [4] and by Heiselberg et al [5].

In nucleus-nucleus ( $AA$ ) collisions relative fluctuations in global observables have been found to be smaller compared to those in  $pp$  collisions. It is suggested that thermal equilibration in  $AA$  collisions makes the fluctuations small. However, the origin of fluctuations and hence the physical information content are quite different in  $pp$  and  $AA$  collisions. While in  $pp$  collisions one hopes to extract quantum mechanical information about the initial state from the event-by-event fluctuations in the final state, in heavy-ion collisions equilibration makes it difficult to achieve this goal, instead the basic aim here has been to relate the event-by-event fluctuations of the final state with the thermodynamic properties at freeze-out.

In this article we present fluctuations in the multiplicities of both charged particles and photons, and in the total transverse energy, over a large range of centralities as measured in the WA98 experiment at the CERN SPS. A major interest has been to search for fluctuations which have a new physics origin, such as those associated with QCD phase transition or from the formation of a DCC.

We compare the fluctuations observed in the experimental data for varying centrality conditions and rapidity intervals to those obtained from different models. In the next section the WA98 experimental set up is described. In section 3 the criteria for the centrality selection appropriate for fluctuation studies are discussed. Multiplicity fluctuations of photons and charged particles and the effect of acceptance are presented in section 4. In section 5, we estimate the multiplicity fluctuations in a participant model and compare to those obtained from data.

Section 6 deals with transverse energy fluctuations. A final discussion and summary is presented in section 7.

## II. EXPERIMENT AND DATA ANALYSIS

In the WA98 experiment at CERN [18], the main emphasis has been on high precision and simultaneous detection of both hadrons and photons. The experimental setup consisted of large acceptance hadron and photon spectrometers, detectors for charged particle and photon multiplicity measurements, and calorimeters for transverse and forward energy measurements. The experiment took data with 158-A GeV Pb beams from the CERN SPS in 1994, 1995, and 1996. The results presented here are from the Pb run in 1996 taken with the magnet (Goliath) turned off. The analysis makes use of the data taken with the photon multiplicity detector (PMD), the silicon pad multiplicity detector (SPMD), the mid-rapidity calorimeter (MIRAC), and the zero degree calorimeter (ZDC).

The circular Silicon Pad Multiplicity Detector (SPMD), used for measuring charged particle multiplicity, was located 32.8 cm from the target. It had full azimuthal coverage in the region  $2.35 \leq \eta \leq 3.75$ . The detector had four overlapping quadrants, each fabricated from a single 300  $\mu\text{m}$  thick silicon wafer. The active area of each quadrant was divided into 1012 pads forming 46 azimuthal wedges and 22 radial bins with pad size increasing with radius to provide a uniform pseudo-rapidity coverage. The intrinsic efficiency of the detector was better than 99 %. During the data taking, 95 % of the pads worked properly. It was nearly transparent to high energy photons, since only about 0.2 % are expected to interact in the silicon. Details of the characteristics of the SPMD can be found in Ref. [19,20].

The photon multiplicity was measured using the preshower photon multiplicity detector (PMD) placed at a distance of 21.5 meters from the target. The detector consisted of 3 radiation length ( $X_0$ ) thick lead converter plates placed in front of an array of square scintillator pads of four different sizes, varying from 15 mm  $\times$  15 mm to 25 mm  $\times$  25 mm, placed in 28 box modules. Each box module had a matrix of 38  $\times$  50 pads which were read out using one image intensifier + CCD camera system. Details of the design and characteristics of the PMD may be found in Ref. [21,22]. The results presented here make use of the data from the central 22 box modules covering the pseudo-rapidity range  $2.9 \leq \eta \leq 4.2$ . The clusters of hit pads, having total ADC content above a hadron rejection threshold were identified as photon-like. Detailed simulations showed that the photon counting efficiencies for the central to peripheral cases varied from 68% to 73%. The purity of the photon sample,  $N_{\gamma\text{-like}}$ , in the two cases varied from 65% to 54%.

The transverse energy was measured with the MIRAC calorimeter [23] placed at 24.7 meters downstream from

the target. It consisted of 30 stacks, each divided vertically into 6 towers, each of size  $20 \times 20 \text{ cm}^2$ , and segmented longitudinally into an electro-magnetic (EM) and a hadronic section. The depth of an EM section was  $15.6X_0$  (equivalent to 51% of an interaction length) which ensured almost complete containment of the electromagnetic energy (97.4% and 91.0% containment calculated for 1 GeV and 30 GeV photons, respectively). The MIRAC was used to measure both the transverse electromagnetic ( $E_T^{em}$ ) and hadronic ( $E_T^{had}$ ) energies in the interval  $3.5 \leq \eta \leq 5.5$  with a resolution of  $17.9\%/\sqrt{E}$  and  $46.1\%/\sqrt{E}$ , ( $E$  in GeV), respectively. The  $E_T$  provides a measure of the centrality of the reaction. Events with large  $E_T$  correspond to very central reactions with small impact parameter and vice versa.

The Zero Degree Calorimeter (ZDC) measured the total forward energy,  $E_F$ , at  $\theta \leq 0.3^\circ$  with a resolution of  $80\%/\sqrt{E} + 1.5\%$ , with  $E$  expressed in GeV.  $E_F$  provides complementary information on the centrality with low  $E_F$  energy deposit corresponding to small impact parameter collisions.

For the results to be presented below, the following sources of errors have been included in the systematic error estimates:

*Errors in  $N_{\gamma\text{-like}}$  :*

(a) The major source of error in  $N_{\gamma\text{-like}}$  is due to the effect of clustering of the pad signals. This error is determined from the simulation by comparing the number of known tracks on the PMD with the total number of photon-like clusters. The result is that the number of clusters exceeds the number of tracks by 3% in the case of peripheral events and by 7% for high multiplicity central events [22].

(b) The uncertainty in the ADC value of the hadron rejection threshold in the PMD leads to an error in the estimation of  $N_{\gamma\text{-like}}$  clusters. The hadron rejection threshold has been set at three times the MIP (minimum ionizing particle) peak. The value of MIP peak was changed by 10% of the peak value (3 ADC) in order to estimate the systematic error. The error in  $N_{\gamma\text{-like}}$  value is 2.5% [22].

(c) The error because of the variation in scintillator pad-to-pad gains is found to be less than 1%.

The combined systematic error on  $N_{\gamma\text{-like}}$  is asymmetric and centrality dependent. The errors are -3.2% and +3.4% for peripheral collisions and -7.1% and +3.0% for central collisions. The errors on  $N_\gamma$ , obtained after correcting for photon counting efficiency and purity of photon-like sample, will be discussed in section V.

*Errors in  $N_{ch}$  :*

The uncertainty in the  $N_{\text{ch}}$  obtained from SPMD has been discussed in detail in Ref. [19]. The total error has been estimated to be about 4%.

#### *Errors in centrality selection through $E_T$ and $E_F$ :*

The centrality of the interaction is determined by the total transverse energy ( $E_T$ ) measured in the MIRAC. The finite resolution in the measurement of  $E_T$  contributes to the systematic error. For the analysis of fluctuation in  $E_T$  which uses MIRAC data directly, the centrality is determined by the forward energy,  $E_F$ . The finite resolution in the measurement  $E_F$  contributes to the systematic error in  $E_T$  fluctuations. These errors are centrality dependent.

#### *Fitting errors :*

The fitting errors associated with the determination of the fit parameters of the multiplicity and transverse energy distributions also contribute to the final systematic error in both the photons and charged particles and transverse energy respectively. The maximum contribution of this error to the fluctuation was found to be 2%.

### III. CENTRALITY SELECTION FOR FLUCTUATION STUDIES

The centrality of the interaction was determined by the total transverse energy measured in the MIRAC. For the part of the analysis where transverse energy data are used for the fluctuation studies, the centrality was determined instead by the forward energy,  $E_F$ , as measured in the ZDC. The centralities are expressed as fractions of the minimum bias cross section as a function of the measured total transverse energy using MIRAC, or total forward energy using the ZDC. Fig. 1(a) and (b) show the minimum bias distributions of  $E_T$  and  $E_F$ , respectively. The arrows in the figures indicate the values of  $E_T$  and  $E_F$  for the top (most central) 1%, 2%, 5%, and 10% of the minimum bias cross section. Predictions from VENUS 4.12 [24] are also shown as solid histograms. This will be discussed in a later section.

The anti-correlation of  $E_T$  and  $E_F$  is shown in 1(c). It illustrates that either  $E_T$  or  $E_F$  can be used nearly equivalently to define the centrality of the reaction.

Fig. 2(a) and 2(b) show the minimum bias distributions for  $\gamma$  - like clusters and charged particles, respectively, for the full acceptances of the two detectors (PMD and SPMD). The multiplicity distributions corresponding to the centrality cuts using the total  $E_T$  for the top 1%, 2%, and 5% of the minimum bias cross section are also shown in the same figures. These distributions have been fitted to Gaussians. The extracted fit parameters are used for the analysis of the fluctuations.

Fig. 3 shows the variation of the mean ( $\mu$ ), standard deviation ( $\sigma$ ), and chi-square per degree of freedom ( $\chi^2/ndf$ ) of the photon and charged particle multiplicity distributions for different centrality bins. Here the centrality class is chosen with increasing width, as 0 - 1%, 0 - 2%, 0 - 3%, ..., 0 - 10%. As expected, the mean value decreases and the sigma increases as we make broader centrality selection to include more of the cross section. From the  $\chi^2/ndf$  values, one observes that the distributions increasingly deviate from Gaussians with increasing width in the centrality selection. For a centrality selection width of greater than 5%, the  $\chi^2/ndf$  rises above 2. The variation of  $\mu$  and  $\sigma$  indicate that the extracted relative fluctuation ( $\omega_X$ ) will grow with the increase in the width of the centrality selection interval. This indicates that the impact parameter fluctuations will dominate as the centrality selection is broadened. From this we conclude that the centrality selections should be made with as narrow bins in  $E_T$  as possible, such that the multiplicity distributions are good Gaussians and the impact parameter fluctuations are minimized. With this in mind we have used centrality selection bins of 2% widths in cross section, taken as, 0 - 2%, 2 - 4%, ..., 62 - 64%.

Fig. 4 shows the variation of  $\mu$ ,  $\sigma$ , and  $\chi^2/ndf$  of the photon and charged particle multiplicity distributions within the full acceptance of the detectors with these narrow bins in centrality. The data presented here cover the region from central (top 2% of the minimum bias cross sections) to peripheral collisions (up to 65% of the minimum bias cross section where the average number of participants is 26). It is seen that both the  $\mu$  and  $\sigma$  values decrease towards peripheral collisions. The  $\chi^2/ndf$  values are mostly in the region between 1.0 and 2.0 over the entire range of centralities considered. This suggests that narrow cross section slices in the  $E_T$  or  $E_F$  distributions are necessary to study the multiplicity fluctuations and minimize the influence from impact parameter fluctuations.

### IV. MULTIPLICITY FLUCTUATIONS AND THE EFFECT OF ACCEPTANCE

The relative fluctuations in multiplicity for  $\gamma$  - like clusters and charged particles have been calculated using the  $\mu$  and  $\sigma$  values from Fig. 4 and Eq. 1. These values are shown in Fig. 5 as functions of centrality, for full coverage of PMD ( $2.9 \leq \eta \leq 4.2$ ) and SPMD ( $2.35 \leq \eta \leq 3.75$ ), respectively. The errors shown in the figures are systematic errors, the sources of which has been already discussed in previous section. For both  $\gamma$  - like clusters and charged particles the relative fluctuations are seen to increase in going from central to peripheral collisions. However, for charged particles the increase is much stronger.

In order to make a direct comparison of the fluctuations of photons and charged particles, the multiplicities

should be studied in the region of common coverage of the detectors in terms of both pseudo-rapidity and azimuthal angle. In a later section we will compare the results obtained from data with those from model calculations for the common coverage. The region of common coverage of the two detectors in the WA98 experiment was 0.85 units in  $\eta$  ( $2.9 \leq \eta \leq 3.75$ ). The general trend of the variation of the Gaussian fit parameters, with the reduced number of particles, for the common coverage is found to be similar to that obtained with full coverage for each detector. Fit parameters  $\mu$ ,  $\sigma$ , and  $\chi^2/ndf$ , as obtained for centrality bins of 2% in width, for the common coverage of the two detectors are shown in Fig. 6. As was the case for the larger acceptance, the  $\mu$  and  $\sigma$  values are seen to decrease towards more peripheral event selection. The  $\chi^2/ndf$  values are reasonable. Using the above values of the Gaussian parameters together with Eq. 1, the relative multiplicity fluctuations were calculated and are shown in Fig. 7. The error shown include the fit errors as well as the other systematic errors discussed earlier. The relative fluctuations for  $\gamma$  – like clusters is seen to be rather constant over the full centrality range with an average value of  $2.2 \pm 0.21$ . In comparison, the relative fluctuations for charged particles is  $1.56 \pm 0.13$  at the most central bin (0 – 2%) increasing to  $2.8 \pm 0.16$  for the least central bin (62-64%).

Following this discussion of the fluctuations in the multiplicity of photons and charged particles for the full acceptance regions and for the regions of common coverage of the photon and charged particle detectors, we now analyze the effect of detector acceptance on the observed fluctuations in more detail. For this we have taken two different  $\eta$  coverage regions for each detector. For the PMD the  $\eta$  ranges chosen are  $3.0 \leq \eta \leq 4.0$  and  $3.25 \leq \eta \leq 3.75$  (with full  $\phi$  coverage). The resulting  $\omega$  values for the two cases are shown in Fig. 8(a). Qualitatively, the variation of the fluctuations with centrality is similar for both coverages, but the magnitude of the relative fluctuations is lower for smaller  $\eta$  coverage.

For the SPMD, the fluctuations were calculated for the rapidity intervals  $2.35 \leq \eta \leq 3.35$  and  $2.65 \leq \eta \leq 3.15$ . These bins have width of one and one half unit in  $\eta$  around mid-rapidity. The results are shown in Fig. 8(b). Qualitatively, the results are again similar to each other with the magnitude of the relative fluctuations decreasing as the coverage in  $\eta$  is decreased.

The decrease in the relative fluctuations as the acceptance is decreased can be understood in terms of a simple statistical picture [25]. Assume that there are  $m$  particles produced in the collision out of which  $n$  particles are accepted randomly into the detector acceptance. In this case, the distribution of  $n$ , will follow a binomial distribution with mean  $mf$  and variance  $mf(1 - f)$  where  $f$  is the fraction of particles accepted. Therefore the fluctuations in the number of particles accepted for a fixed ( $m$ ) number of particles produced is  $(1 - f)$ . In principle  $m$  can have an arbitrary distribution as given by  $P(m)$  with

known first and second moments. The fluctuations in the  $n$  accepted particles out of the  $m$  particles produced is then given as:

$$\omega_n = 1 - f + f\omega_m \quad (2)$$

Thus considering the fluctuations in one unit of  $\eta$  as  $\omega_m$  we can calculate the expected fluctuations for one half unit of  $\eta$  using the above equation. Here  $f$  corresponds to the ratio of the total number of particles accepted in one half unit of  $\eta$  coverage to that accepted over one unit in  $\eta$ . For the acceptance regions used, the average value of  $f$  for photons is about 0.52 and that of charged particles is about 0.54. Using these values in Eq. 2 we can calculate the expected fluctuations for half unit of  $\eta$  coverage from the results for one unit of  $\eta$  coverage, under the assumption of a binomial sampling. As shown in Fig. 8 the empirical calculations almost exactly reproduce the observed result in the narrower acceptance window for charged particles and agrees reasonably well within the quoted errors for photons.

## V. ESTIMATION OF FLUCTUATIONS IN A PARTICIPANT MODEL

In a picture where the nucleus-nucleus collision is thought of as the sum of contributions from many sources created in the early stage of the interaction, the variance of the distribution of any observable has contributions from:

- the fluctuations in the number of sources, largely due to different impact parameters. Even if the impact parameter window is narrowed, density fluctuations within the nucleus will make this contribution non-zero.
- the fluctuations in the number of particles produced by each source. Quantum fluctuations in the  $NN$  cross section can lead to such effects.
- the fluctuations due to any dynamical process or critical behavior in the evolution of the system.

The contribution from the first two effects leads to fluctuations in the number of participant nucleons which may be related to the initial size of the interacting system before it thermalizes. Resonance decays have also been shown to increase the multiplicity fluctuations by a large factor [4,5].

Following a simple participant model [5,15,16,26,27], the particle multiplicity (of photons or charged particles),  $N$ , may be expressed as :

$$N = \sum_{i=1}^{N_{\text{part}}} n_i \quad (3)$$

where  $N_{\text{part}}$  is the number of participants and  $n_i$  is the number of particles produced in the detector acceptance by the  $i^{\text{th}}$  participant. On an average, the mean value of  $n_i$  is the ratio of the average multiplicity in the detector coverage to the average number of participants, i.e.,  $\langle n \rangle = \langle N \rangle / \langle N_{\text{part}} \rangle$ .

Thus the fluctuations in  $N$  will have contributions due to fluctuations in  $N_{\text{part}}$  ( $\omega_{N_{\text{part}}}$ ) and also due to the fluctuations in the number particles produced per participant ( $\omega_n$ ). Again, the fluctuations of  $n$  given as  $\omega_n$ , will have a strong dependence on the acceptance of the detector. In the absence of correlations between the  $n_i$ 's, the multiplicity fluctuations,  $\omega_N$ , can be expressed as

$$\omega_N = \omega_n + \langle n \rangle \omega_{N_{\text{part}}} \quad (4)$$

Comparison of data with the results of such model calculations might reveal the extent to which the principle of superposition of nucleon-nucleon (NN) interactions is valid in the case of heavy ion collisions. The participant model is expected to hold reasonably well for peripheral collisions where there are only few NN collisions, while for central collisions the particle production gets affected by NN scattering, rescatterings between produced particles, energy degradation, and other effects. Next we discuss the calculation of each of the terms in Eq. 4.

#### A. Calculation of $\omega_{N_{\text{part}}}$

The impact parameter fluctuations are reflected in the fluctuations in the number of participants. We have estimated this contribution using the VENUS 4.12 event generator with default setting. A set of 100K minimum bias Pb+Pb events at 158.4 GeV was generated for calculation of the number of participants. To match the centrality selection of the reaction in simulation to that in data, we have carried out a fast simulation in which  $E_T$  from VENUS was calculated within MIRAC coverage taking the resolution factors for the hadronic and electromagnetic energies of MIRAC into account. The corresponding  $E_T$  distributions for VENUS are shown as the solid curve in Fig. 1(a). It is seen that the agreement with data is quite reasonable.

The distributions of  $N_{\text{part}}$  for the same narrow (2%) bins of centrality, as discussed above for the data, are well described by Gaussian distributions. Fig. 9 shows the variation of  $\mu$ ,  $\sigma$ ,  $\chi^2/ndf$ , and relative fluctuation  $\omega_{N_{\text{part}}}$  calculated from the fit parameters with the 2% bins in centrality. One can see that the relative fluctuation in the number of participants,  $\omega_{N_{\text{part}}}$ , is around 1. The statistical errors are small and are within the size of the symbols.

The systematic errors shown in the figures, have contribution from the following sources, which have been added in quadrature.

- Nucleon density distribution: In order to estimate the error due to this we have calculated the number of participants from VENUS (as shown in the figure) and those from FRITIOF. The difference for each centrality bin was considered as representative of the error [28].
- Finite resolution of  $E_T$ : Systematic errors due to this were calculated by varying the centrality as per the MIRAC resolution [22].
- Fitting errors: Errors associated with the determination of the fit parameters of the Gaussian distributions also contribute to the final systematic error in the number of participants.

The quantity  $\langle n \rangle$  is equal to the ratio of the mean charged particle (or photon) multiplicity for a given acceptance to the mean number of participants for the same centrality bin. Thus the contribution from the term  $\langle n \rangle \omega_{N_{\text{part}}}$  to the total fluctuations (Eq. 4) can be easily obtained.

#### B. Calculation of $\omega_n$

This term gives the fluctuations in the number of particles produced per participant. It has a strong dependence on acceptance as given earlier in Eq. 2 and shown in Fig. 8. To calculate  $\omega_n$  as per Eq. 2 we next obtain the terms  $f$  and  $\omega_m$ . The quantity  $f$  is the ratio of the number of particles per participant accepted within the acceptance of the detector ( $\langle n \rangle$ ) to the total number of particles produced per participant ( $\langle m \rangle$ ). The value of  $\langle n \rangle$  for each centrality bin and for a given acceptance can be calculated as discussed in the preceding section. To obtain the value of  $\langle m \rangle$  we make use of the data existing in the literature for nucleon-nucleon (NN) collisions. As discussed in Refs. [29,30] the mean number of charged particles and photons produced in nucleon-nucleon collisions can be parametrized as a function of cms energies ( $\sqrt{s}$  from 2 GeV to 500 GeV) in the following manner :

$$\langle N_{\text{ch}} \rangle^{NN} = -4.7(\pm 1.0) + 5.2(\pm 0.8)s^{0.145(\pm 0.01)} \quad (5)$$

$$\langle N_{\gamma} \rangle^{NN} = -9.9(\pm 2.1) + 8.5(\pm 1.9)s^{0.113(\pm 0.015)} \quad (6)$$

For the 158.4 GeV SPS energy discussed here this parameterization gives the average charged particle multiplicity to be 7.2 with the corresponding number for photons being 6.3. Thus the average charged particle and photon multiplicities per participant are 3.6 and 3.15 respectively.

In addition,  $\sigma$  for the charged particle multiplicity in nucleon-nucleon collisions shows a linear dependence with the average charged particle multiplicity as  $0.576(\langle N_{\text{ch}}^{NN} \rangle - 1)$ , as given in Ref. [30].

This can be used to calculate  $\omega_m$ , which is given as:

$$\omega_m = 0.33 \frac{(\langle N_{\text{ch}} \rangle - 1)^2}{\langle N_{\text{ch}} \rangle} \quad (7)$$

For charged particles at SPS energies this gives a value of  $\omega_m = 1.8$ . However, for photons this number is not known since there is no similar parameterization. In the absence of such a parameterization of  $\sigma$  for photons we will also assume that  $\omega_m = 1.8$  for the photon multiplicity. Fluctuations of photons, in principle, are expected to be similar to those for charged particles. This is because the majority of photons come from decay of  $\pi^0$  and while the majority of charged particles are charged pions ( $\pi^\pm$ ).

From the values of  $\langle n \rangle$ ,  $\langle m \rangle$ , and  $\omega_m$  for a given acceptance and centrality, the term  $\omega_n$  can then be calculated.

### C. Comparison of data to model calculations

We first compare the experimental results of multiplicity fluctuations to those of the calculations using the participant model in the common coverage of PMD and SPMD. Fig. 10 shows a comparison of the fluctuation in charged particles from data to that obtained from the calculations using the model described above. The results are plotted as a function of the number of participants. The horizontal errors on the number of participants are shown only on the data points. The error on  $\omega$  calculated in the model is mainly due to the error on the mean number of charged particles in nucleon-nucleon interactions, the error in the number of participants calculated, and the uncertainty in the simulation of the calculated transverse energy. For clarity of presentation we have given results corresponding to alternate 2% centrality bins, i.e 0–2%, 2–4%, ..., 62–64%. The results from VENUS are also shown in form of solid line in Fig. 10, and are found to remain almost constant over the entire centrality range. Charged particle fluctuations determined from data and the participant model decrease in going from peripheral to central collisions, although the dependence on centrality is weaker for the model calculation.

Fig. 11 shows fluctuations in the  $\gamma$ -like clusters as well as  $N_\gamma$  after the correction. The results, plotted as a function of the number of participants, are compared to those of the participant model calculations for photons and results from VENUS. Using the estimated values of efficiency ( $\epsilon_\gamma$ ) and purity ( $f_p$ ), the number of photons in an event is calculated by using the relation:

$$N_\gamma = \frac{f_p}{\epsilon_\gamma} N_{\gamma\text{-like}} \quad (8)$$

The photon counting efficiency in PMD varies from 68% to 73% for central to peripheral collisions. The purity of the measured photon sample varies from 65% to 54% for central to peripheral collisions.

The systematic errors associated with  $N_{\gamma\text{-like}}$  have already been discussed in section II. The additional errors in the conversion from  $N_{\gamma\text{-like}}$  to  $N_\gamma$  are mainly due to errors in estimation of photon counting efficiency and purity. These sources of these errors are given below:

- Event-by-event variation in photon counting efficiency ( $\epsilon_\gamma$ ) and purity of photon sample ( $f_p$ ). These have been found to vary from 3% to 6% for central to peripheral collisions.
- The purity factor depends on the ratio of the number of photons and charged particles within the PMD coverage. The systematic error associated with this ratio has been studied by using the FRITIOF [31] event generator in addition to VENUS. The average photon multiplicity estimated by using FRITIOF is found to be higher by about 4% in peripheral and by 1% in central collisions, compared to the values obtained using VENUS.
- The photon counting efficiency determined in the present case relies on the energy spectra of photons as given by the VENUS event generator. As the conversion probability for low energy photons falls sharply [32] with decreasing energy below 500 MeV, the estimate of  $\epsilon_\gamma$  may be affected if the energy spectra in the actual case is different. Photon energy spectra have been measured by the WA98 lead glass calorimeter. By extrapolating these measured spectra to the PMD acceptance we have estimated the photon counting efficiencies for different eta bins and centralities. These results turn out to be lower compared to those obtained from VENUS by 2-9% for central events and 3-13% for peripheral events, the smaller value corresponds to larger pseudo-rapidity region of the PMD acceptance. The average difference in efficiencies within the PMD acceptance are 6% for central and 9% for peripheral collisions. These differences add to the systematic errors on the photon counting efficiency.

The total systematic error on the multiplicity of photons ( $N_\gamma$ ) are -6.7% and +12.5% for peripheral collisions and -8.0% and +9.0% for central collisions.

The fluctuations in the number of photons have been estimated from the fluctuations in the number of photon-like clusters by using Eq. 8:

$$\omega_\gamma = \frac{f_p}{\epsilon_\gamma} \omega_{\gamma\text{-like}} \quad (9)$$

These results are shown in Fig. 11. It is observed that the relative fluctuations of photons from the data are in reasonable agreement with those obtained from VENUS. However, the results for photons from the participant model are somewhat higher than those from the experimental data.

## VI. TRANSVERSE ENERGY FLUCTUATIONS

Relativistic nuclear collisions are often described within the participant-spectator picture in which nuclei are spheres that collide with a definite impact parameter. The overlapping volume which participate in the reaction are violently disrupted while the remaining spectator volumes shear off and suffer comparatively mild excitations. The magnitude of the  $E_T$  produced depends on the bombarding energy and the participant volume or equivalently the number of participating nucleons. The cross section for a specific value of  $E_T$  production depends to a large extent on the geometric probability of a given impact parameter. Therefore impact parameter fluctuations are expected to lead to fluctuations in  $E_T$ .

Corroboration of the participant-spectator picture comes from the strong anti-correlation of  $E_T$  with the energy observed in the zero degree calorimeter,  $E_F$  as shown in the Fig. 1(b). The smaller the impact parameter, the larger is the participant volume and  $E_T$ , but the smaller is the spectator volume and  $E_F$ .  $E_T$  also correlates strongly with the produced particle multiplicity. The  $d\sigma/dN_{ch}$  and  $d\sigma/dN_{\gamma\text{-like}}$  spectra have virtually the same shape as  $d\sigma/dE_T$  (Fig. 2(a) and Fig. 2(b)).

The study of the average total  $E_T$  as measured in the WA98 experiment and its scaling behavior with the number of participants have been discussed earlier in detail in Ref. [28]. Here we concentrate on the second moment, and study the fluctuations in  $E_T$  as was done for  $N_{\gamma\text{-like}}$  and  $N_{ch}$ . For this analysis we have again taken 2% width bins in centrality using the forward energy as measured by the ZDC. Due to the poorer resolution in centrality selection of the ZDC for peripheral collisions, we present the results only up to the 50% centrality class.

The  $E_T$  distribution for the top 2% of the minimum bias cross section is shown in Fig. 12. The solid curve shows a Gaussian fit to the distribution. The  $\mu$ ,  $\sigma$  and  $\chi^2/ndf$  values for such distributions at centrality bins varying from 0-2% to 48-50% have been extracted and are shown in Fig. 13. The  $\chi^2/ndf$  values are seen to be between 1 and 2, which indicates that the distributions are well described by Gaussians. The fluctuations in  $E_T$  have been calculated by using Eq. 1 and are shown in Fig. 14. The relative fluctuations are observed to increase in going from central to peripheral collisions.  $E_T$ , measured by the MIRAC was used in the online trigger to define the most central event sample with a threshold which occurred in the region of the top 14% – 18% of the total cross section. This region is not analyzed to avoid trigger bias effects in the measured  $E_T$  distribution.

$E_T$  has a strong correlation with the number of participant nucleons or the number of effective collisions they undergo [33]. In an attempt to understand the fluctuations in terms of the number of participant nucleons, the VENUS event generator has been used to determine the ratio  $\mu(E_T)/\mu(N_{part})$  as a function of centrality. The  $\mu(E_T)$  per participant has been found to be

$\sim 1.1\text{GeV} \pm 0.2$ . This is shown in Fig. 15. The main sources of error here are due to the uncertainty in the calculation of the number of participants and the finite resolution of the calorimeters. Similar results were also obtained from WA80 and HELIOS collaborations Ref. [11,12]. While the WA80 Collaboration has shown that  $E_T$  per participant is independent of projectile, target, and centrality but depends only on the number of wounded nucleons and the beam energy, the WA98 Collaboration has shown that transverse energy does deviate from a linear dependence on the number of participants for Pb+Pb collisions [28].

The relative fluctuations in transverse energy can be analyzed in a participant picture similar to that employed in the case of photons and charged particles [33]. An expression similar to Eq. 4 can be obtained, where the first term depends on the fluctuations in the transverse energy deposited by each particle produced per participant nucleon, with the second term coming from impact parameter fluctuations within the acceptance of the detector. Since the first term depends greatly on the detector characteristics, we compare the transverse energy fluctuations in data to those obtained from a fast simulation of the MIRAC and ZDC characteristics in VENUS in which the energy resolution for each particle was applied separately when computing the total transverse energy [23]. Fig. 1(a and b) shows the comparison of the simulated  $E_T$  and  $E_F$  distributions with those from data. The agreement is seen to be quite reasonable.

Fig. 16 shows the comparison of  $E_T$  fluctuations from data to those obtained from simulated events using VENUS. The fluctuations are plotted as a function of the mean number of participants in various 2% bins of centrality obtained from  $E_F$ . Errors shown in the data are mainly due to uncertainties in the determination of number of participants and the finite energy resolution of the calorimeters as discussed earlier. It is seen that the fluctuation in data are systematically smaller than those obtained from VENUS. As discussed in Ref. [33] many effects like energy-momentum degradation of nucleonic objects in successive scatterings and short range correlations between nucleons in a nucleus may be responsible for the decrease in fluctuations in  $E_T$  of data as compared to those obtained from simulations in VENUS. The role of re-scattering has also to be understood in this context.

## VII. SUMMARY

A detailed event-by-event study of fluctuations in the multiplicities of charged particles and photons and transverse energy has been carried out using data from the WA98 experiment. This has been done varying both the centrality and rapidity intervals. It is observed that the relative fluctuations increase with increase in the impact parameter interval. Hence it is important to control the impact parameter dependence by studying narrow bins in

centrality. For 2% centrality bins, within which the distributions of charged particle and photon multiplicities, as well as the transverse energy, are well-described by Gaussians, the contribution from impact parameter fluctuations is around one, as expected. The fluctuations in multiplicities and  $E_T$  are found to increase in going from central towards peripheral events. A decrease in acceptance has been found to result in a decreased multiplicity fluctuations. Using a simple statistical analysis one can explain the observed decrease in a smaller acceptance knowing the fluctuations in a larger acceptance window. The observed centrality dependence of the multiplicity fluctuations of charged particles have been found to agree reasonably well with results obtained from a simple participant model which takes into account impact parameter fluctuations from VENUS and multiplicity fluctuations from  $NN$  data, within the quoted systematic errors. For photons the fluctuations are found to be slightly lower compared to those obtained from the participant model.

Similar calculations have been performed for the transverse energy and multiplicity distributions using VENUS. The transverse energy fluctuations from experimental data are found to be smaller than those observed in VENUS. On the other hand, after corrections for charged particle contamination in the photon-like clusters, the relative fluctuations of photons appear to be in rather good agreement with VENUS.

#### Acknowledgements

We wish to express our gratitude to the CERN accelerator division for the excellent performance of the SPS accelerator complex. We acknowledge with appreciation the effort of all engineers, technicians and support staff who have participated in the construction of this experiment.

This work was supported jointly by the German BMBF and DFG, the U.S. DOE, the Swedish NFR and FRN, the Dutch Stichting FOM, the Polish KBN under Contract No. 621/E-78/SPUB-M/CERN/P-03/DZ211/, the Grant Agency of the Czech Republic under contract No. 202/95/0217, the Department of Atomic Energy, the Department of Science and Technology, the Council of Scientific and Industrial Research and the University Grants Commission of the Government of India, the Indo-FRG Exchange Program, the PPE division of CERN, the Swiss National Fund, the INTAS under Contract INTAS-97-0158, ORISE, Grant-in-Aid for Scientific Research (Specially Promoted Research & International Scientific Research) of the Ministry of Education, Science and Culture, the University of Tsukuba Special Research Projects, and the JSPS Research Fellowships for Young Scientists. ORNL is managed by UT-Battelle, LLC, for the U.S. Department of Energy under contract DE-AC05-00OR22725. The MIT group has been supported by the US Dept. of Energy under the cooperative agreement DE-FC02-94ER40818.

- 
- [1] L. van Hove, Phys. Lett. **B118**, 138 (1982); H. Heiselberg, Phys. Rep. **351**, 161 (2001); E.V. Shuryak, Phys. Lett. **B423**, 9 (1998); M. Gazdzicki and S. Mrowczynski, Z. Phys. **C57**, 127 (1992); S. Mrowczynski, Phys. Rev. C **57**, 1518 (1998); Phys. Lett. **B430** 9 (1998).
  - [2] Proceedings of *Quark Matter '99*, Nucl. Phys A **661** (1999).
  - [3] Proceedings of *Quark Matter '2001*, To appear in Nucl. Phys A.
  - [4] M. Stephanov, K. Rajagopal and E. Shuryak, Phys. Rev. Lett. **81**, 4816 (1998); Phys. Rev. D **61**, 114028 (1999).
  - [5] G. Baym and H. Heiselberg, Phys. Lett. **B469**, 7 (1999).
  - [6] M.Asakawa, U.Heinz, and B.Müller, Phys. Rev. Lett. **85**, 2072 (2000).
  - [7] S. Jeon and V. Koch Phys. Rev. Lett. **83**, 5435 (1999); S. Jeon and V. Koch, Phys. Rev. Lett. **85**, 2076 (2000).
  - [8] L. van Hove, Z. Phys. **C21**, 93 (1984); J.I. Kapusta and A.P. Vischer, Phys. Rev. **C52**, 2725 (1995).
  - [9] K. Rajagopal and F. Wilczek, Nucl. Phys. **B399**, 395 (1993); Nucl. Phys. **B404**, 577 (1993); J.D. Bjorken, Int. J. Mod. Phys. **A7**, 4189 (1992); T.C. Brooks et al., (Minimax Collaboration), Phys. Rev. **D61**, 032003 (2000); J. -P. Blaizot and A. Krzywicki, Phys. Rev. **D46**, 246 (1992).
  - [10] M.M. Aggarwal et al., (WA98 Collaboration) Phys. Rev. **C64**, 011901R (2001).
  - [11] T. Akesson et al., Z. Phys. **C38**, 383 (1988).
  - [12] T. Akesson et al., Phys. Lett. **B214**, 214 (1988).
  - [13] T. Alber et al., (NA49 Collaboration) Phys. Rev. Lett. **75**, 3814 (1995).
  - [14] H. Appelshauser et al., (NA49 Collaboration), Phys. Lett. **B459**, 679 (1999); G. Roland, Nucl. Phys. **A638**, 91c (1998).
  - [15] G. Baym et al., Phys. Lett. **B219**, 205 (1989).
  - [16] F. Corriveau et al., (NA34 Collaboration), Z. Phys. **C38**, 15 (1988); J. Schukraft et al., (NA34 Collaboration), Z. Phys. **C38**, 59 (1988).
  - [17] R. Albrecht et al., Z. Phys. **C45**, 31 (1989).
  - [18] *Proposal for a Large Acceptance Hadron and Photon Spectrometer*, Preprint CERN/SPSLC 91-17, SP-SLC/P260.
  - [19] M.M. Aggarwal et al., (WA98 Collaboration), Phys. Lett. **B420**, 169 (1998).
  - [20] W.T. Lin et al., Nucl. Instrum. Meth. **A389**, 415 (1997).
  - [21] M.M. Aggarwal et al., Nucl. Instrum. and Methods in Phys. Res. **A424**, 395 (1999).
  - [22] M.M. Aggarwal et al., (WA98 Collaboration), Phys. Lett. **B458**, 422 (1999).
  - [23] T. C. Awes et al., Nucl. Instrum. Methods Phys. Res. Sect. A **279**, 497 (1989).
  - [24] K. Werner, Phys. Rep. **C232**, 87 (1993).
  - [25] D.P. Mahapatra, B. Mohanty and S.C. Phatak, e-print:nucl-ex/0108011; To be published in Int. J. Mod. Phys. **A**.
  - [26] Rudolph C. Hwa, Phys. Lett. **B201**, 165 (1988).

- [27] A. Giovannini and L. Van. Hove, Z. Phys. **C30**, 391 (1986).
- [28] M.M. Aggarwal et al., (WA98 Collaboration), Eur. Phys J. **C18**, 651 (2001).
- [29] G.J. Alner et al., (UA5 Collaboration), Phys. Rep. **C154**, 247 (1987).
- [30] J. Whitmore, Phys. Rep. **C27**, 188 (1976); J. Whitmore, Phys. Rep. **C10**, 274 (1974).
- [31] B. Nilsson-Almqvist, E. Stenlund, Comp. Phys. Comm. **43** (1987) 387.
- [32] M.M. Aggarwal et al., Nucl. Instrum. and Methods in Phys. Res. **A372**, 143 (1996).
- [33] Gordon Baym et al., Phys. Lett. **B190**, 29 (1987); A.D. Jackson and H. Bogglid, Nucl. Phys. **A470**, 669 (1987).

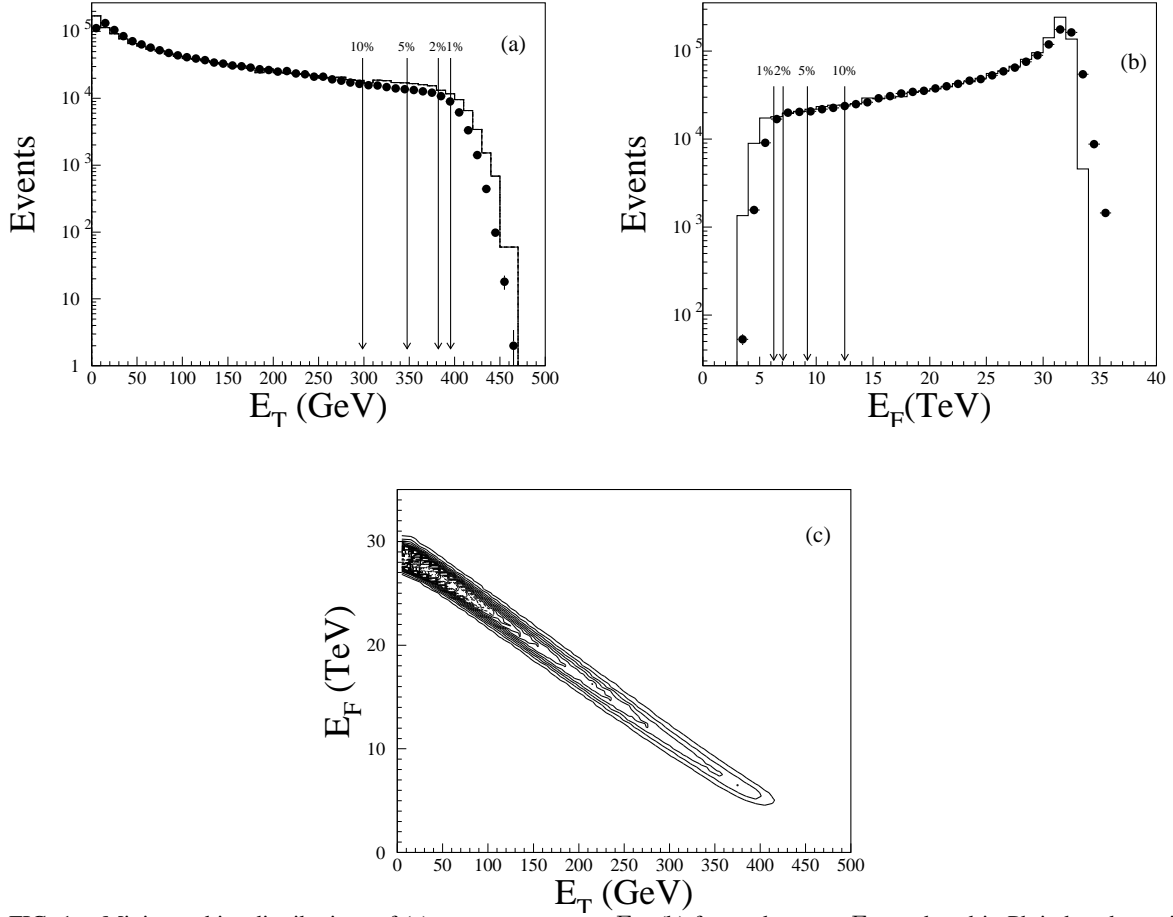


FIG. 1. Minimum bias distributions of (a) transverse energy  $E_T$ , (b) forward energy  $E_F$  produced in Pb induced reactions at  $158\text{-}A$  GeV on Pb. Solid histograms show the results obtained from VENUS event generator. (c) shows the anti-correlation of measured total transverse energy,  $E_T$ , and forward energy,  $E_F$ .

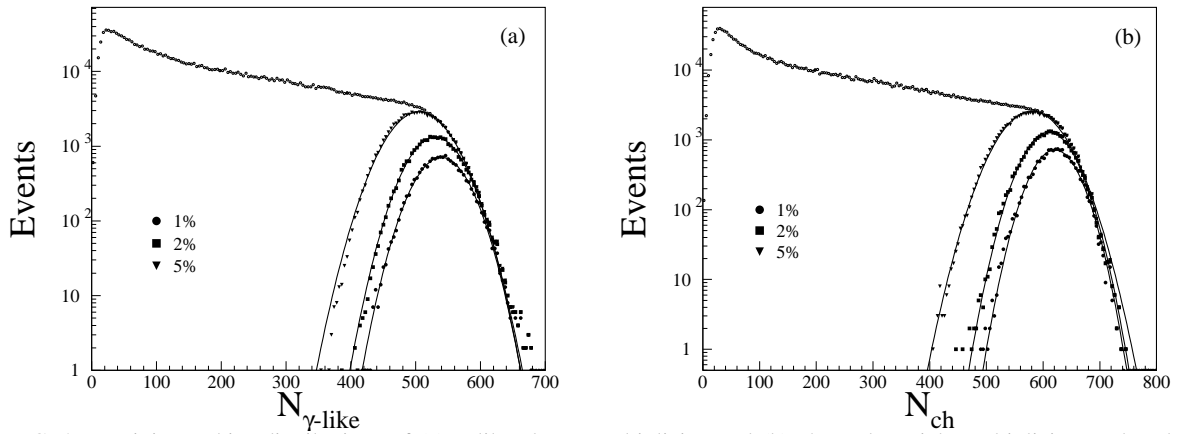


FIG. 2. Minimum bias distributions of (a)  $\gamma$ -like cluster multiplicity, and (b) charged particle multiplicity produced in Pb induced reactions at  $158\text{-}A$  GeV on Pb. The multiplicity distributions for the top 1%, 2%, and 5% most central events are also shown and fitted to Gaussian distributions.

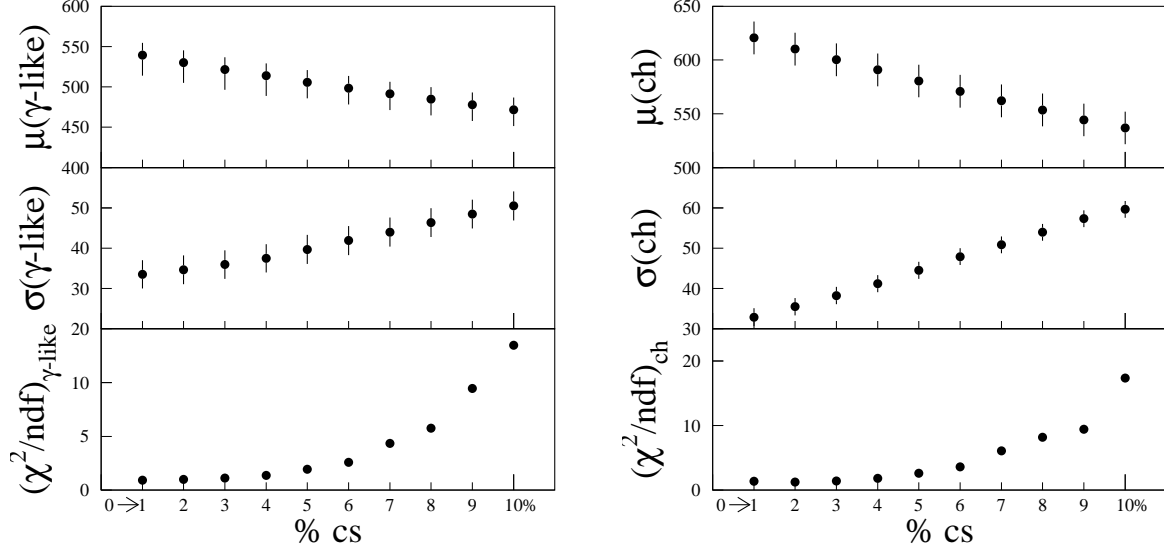


FIG. 3. Gaussian fit parameters of the multiplicity distributions of  $\gamma$ -like clusters and charged particles for increasing centrality bins of increasing width. The centrality selection has been made by increasing the widths of  $E_T$  bins corresponding to 0 – 1%, 0 – 2%, 0 – 3%, ..., 0 – 10% of the minimum bias cross section.

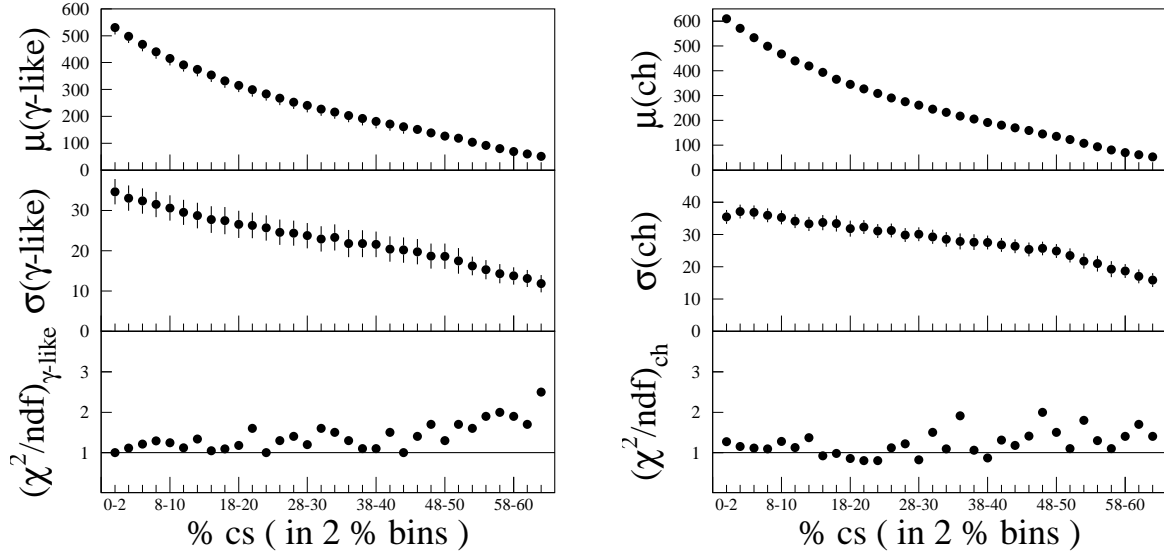


FIG. 4. Gaussian fit parameters of the multiplicity distributions of  $\gamma$  – like clusters and charged particles as a function of centrality. The centrality selection has been made by selecting 2% bins in minimum bias cross section, *viz.*, 0 – 2%, 2 – 4%, 4 – 6%, ..., 62 – 64%. The multiplicity distributions for these centrality bins are near perfect Gaussians as can be seen from the  $\chi^2/ndf$  values.

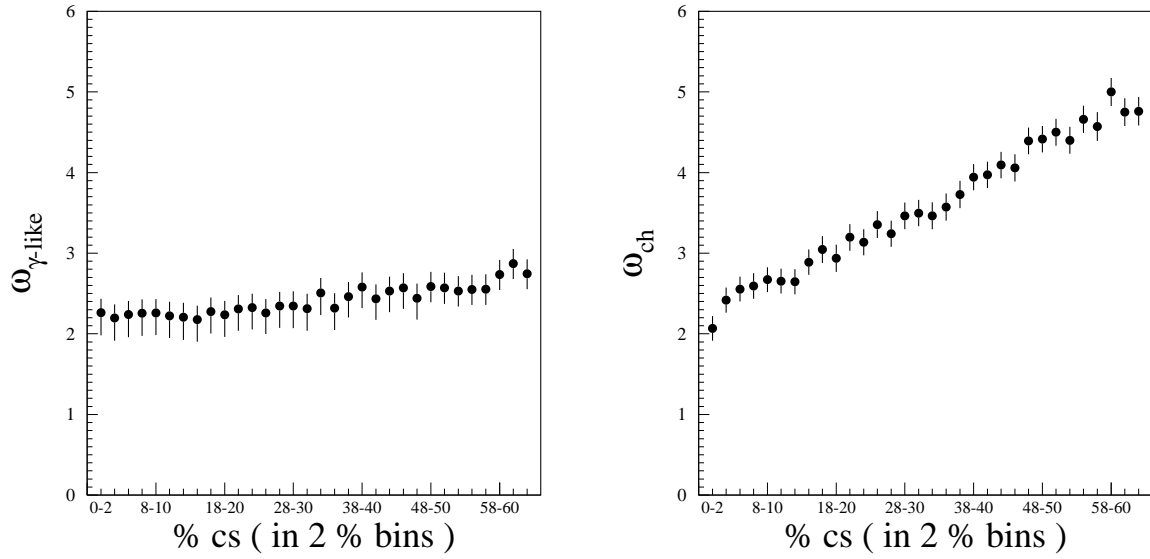


FIG. 5. Fluctuations of the multiplicity of  $\gamma$ -like clusters and charged particles within the full coverage of PMD and SPMD for various 2% bins of the minimum bias cross section.

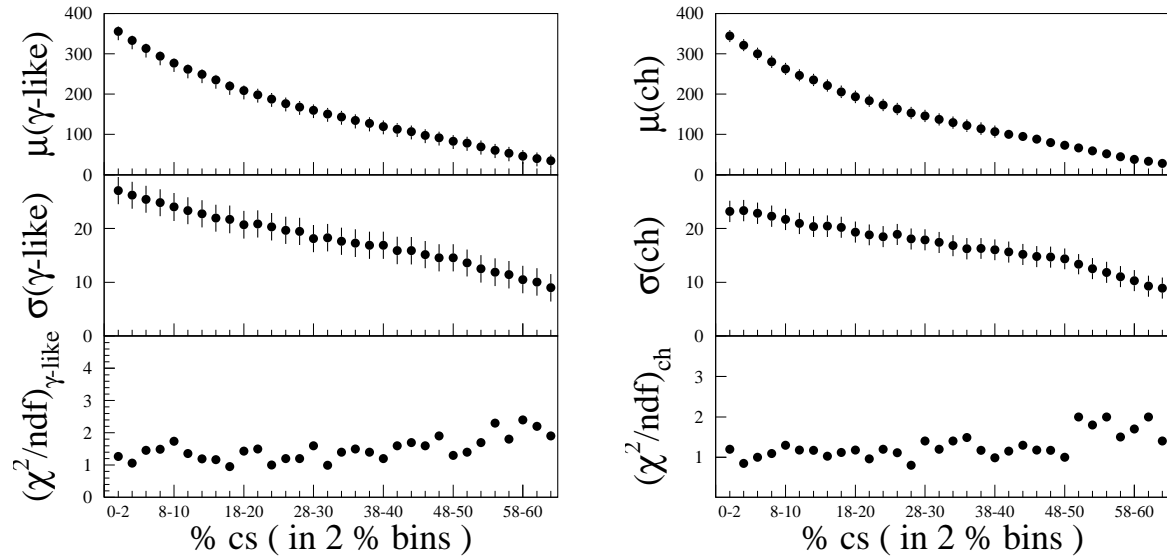


FIG. 6. Centrality dependence of the Gaussian fit parameters of the multiplicity distribution of  $\gamma$ -like clusters and charged particles within the common coverage of PMD and SPMD.

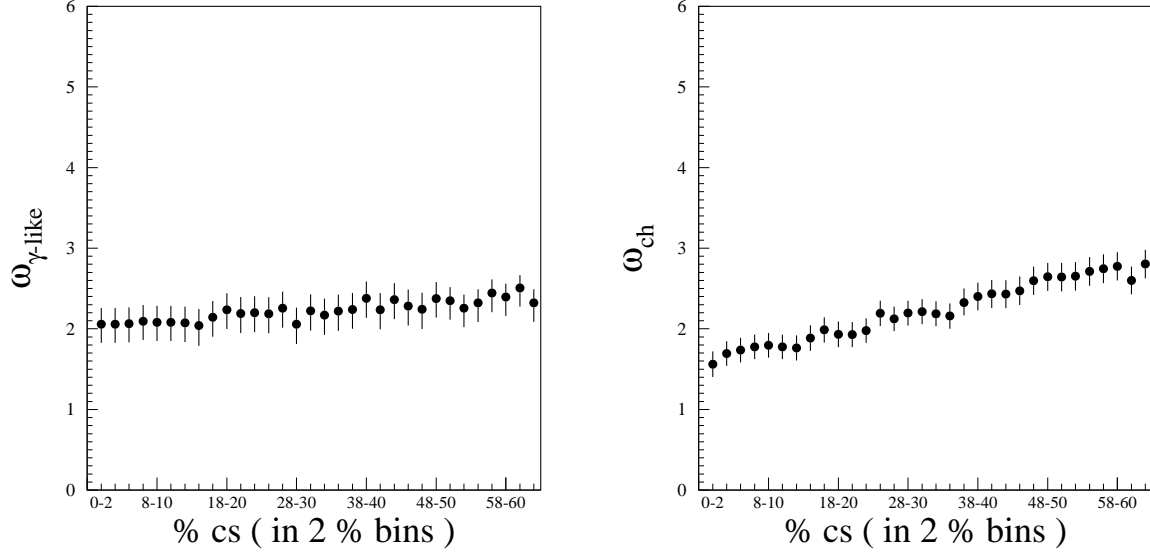


FIG. 7. Centrality dependence of the fluctuations of the multiplicity of photons and charged particles within the common coverage of the PMD and SPMD.

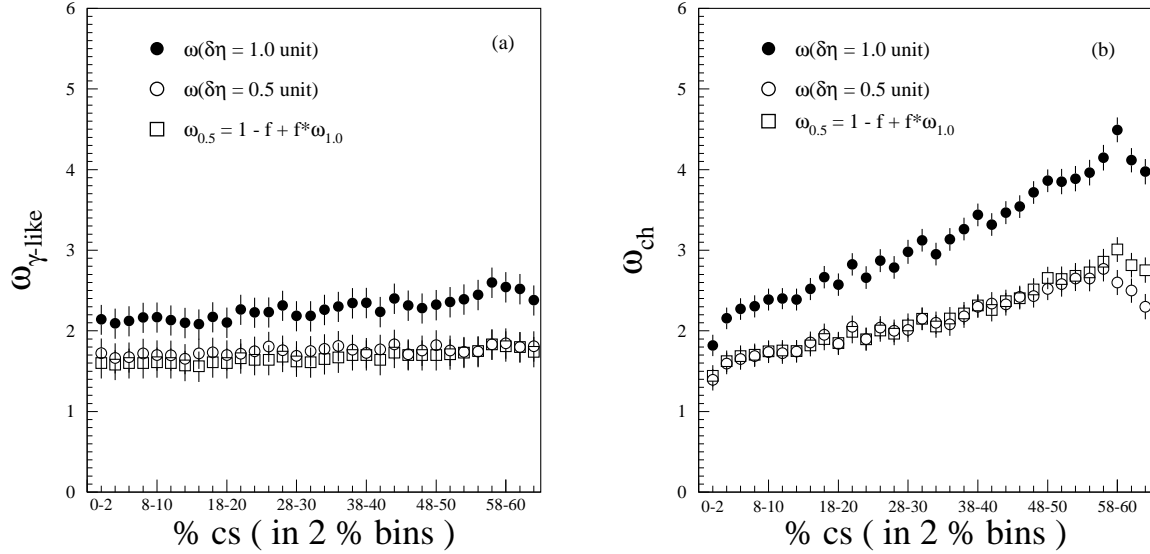


FIG. 8. Multiplicity fluctuations of photons and charged particles for two  $\eta$  acceptance selections. The open squares represent estimated values fluctuations in 0.5 unit of  $\delta\eta$  from the observed fluctuations in 1.0 unit of  $\delta\eta$ .

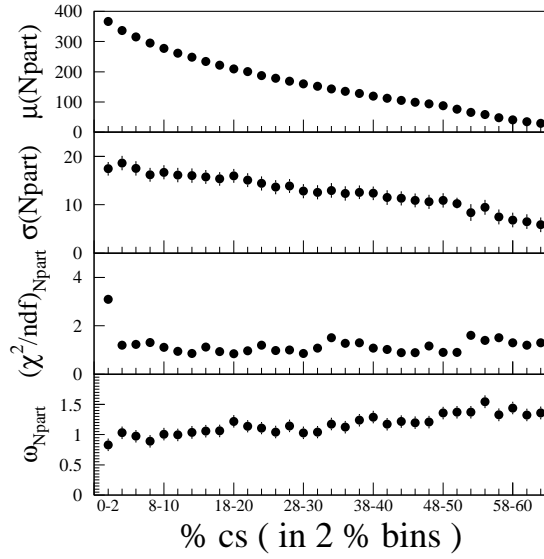


FIG. 9. Variation of  $\mu$ ,  $\sigma$ , and  $\chi^2/ndf$  of the distribution of the number of participants as a function of centrality.

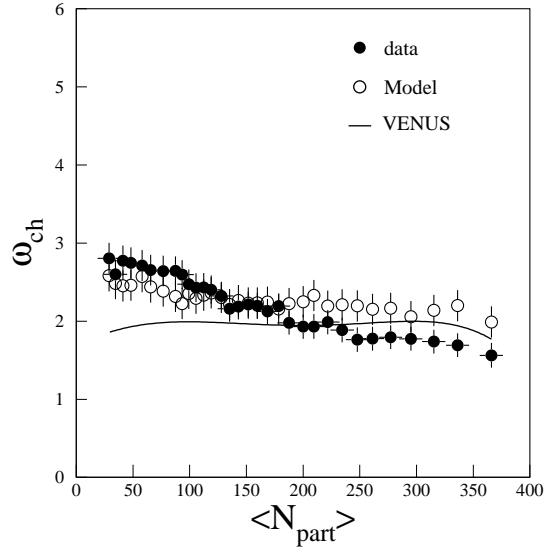


FIG. 10. The relative fluctuations,  $\omega_{ch}$ , of the charged particle multiplicity as a function of number of participants. The experimental data are compared to calculations from a participant model and those from VENUS event generator.

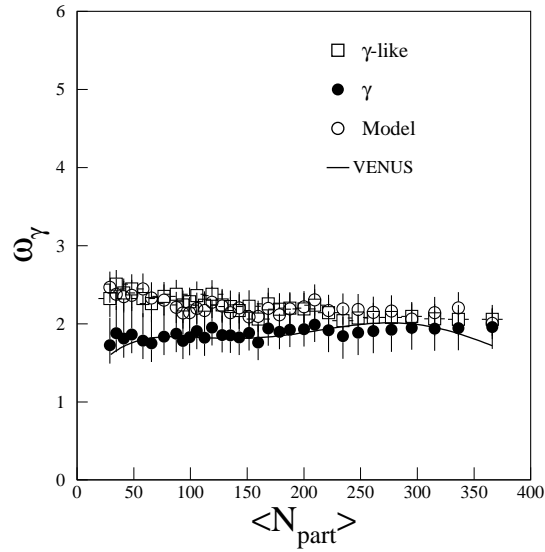


FIG. 11. The relative fluctuations,  $\omega_\gamma$  of photons as a function of number of participants. The data presented show the fluctuations in  $\gamma$  - *like* clusters and photons after correction for efficiency and purity. These are compared to calculations from a participant model and those from VENUS event generator.

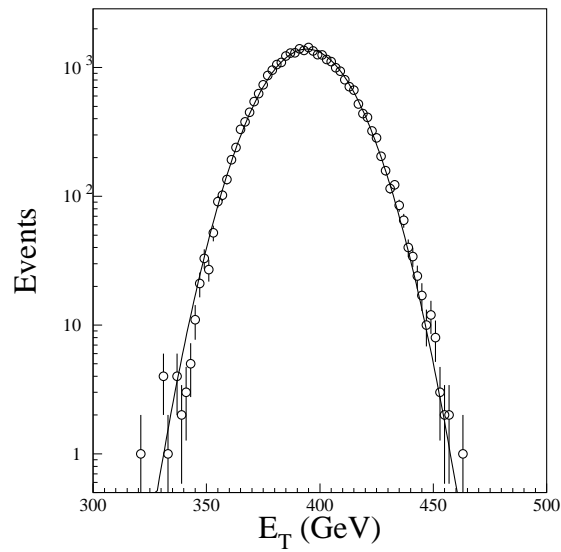


FIG. 12. The transverse energy distribution for the top 2% of the minimum bias cross section.

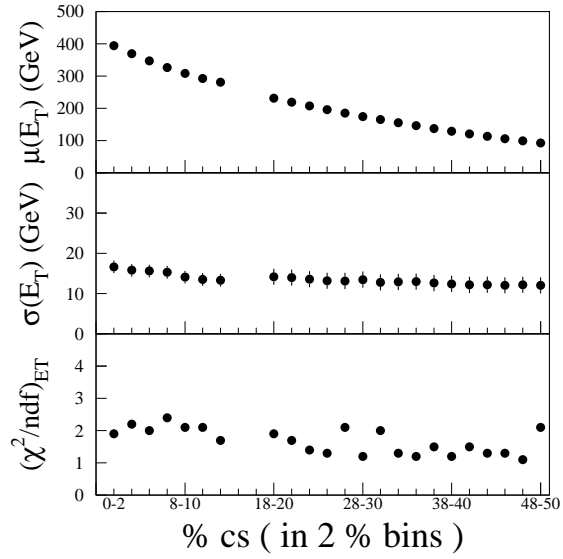


FIG. 13. Centrality dependence of  $\mu$ ,  $\sigma$ , and  $\chi^2/ndf$  of the transverse energy distribution. The centrality selection is based on  $E_F$  measured with the ZDC.

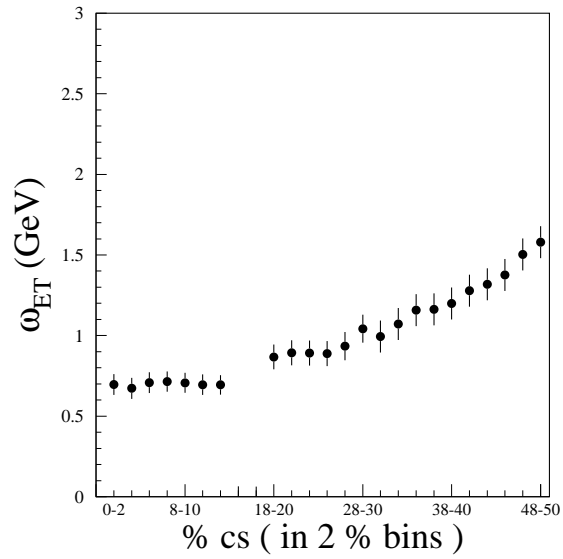


FIG. 14. Centrality dependence of the relative fluctuations in total transverse energy,  $E_T$ , with centrality selected by  $E_F$ .

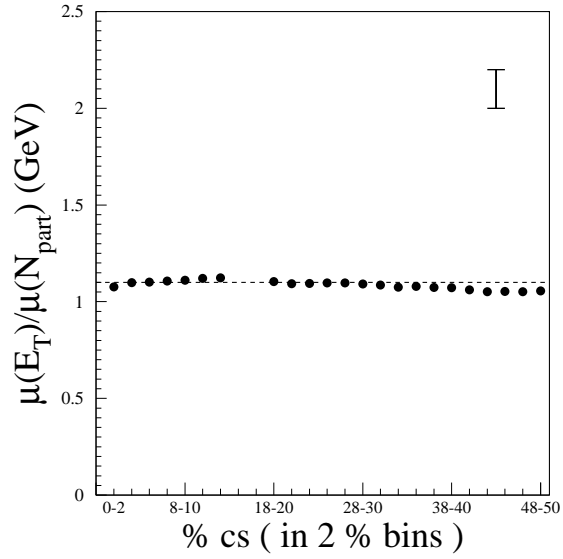


FIG. 15.  $E_T$  per participant as a function of centrality. The vertical solid line indicates the estimated systematic error in  $E_T$  per participant.

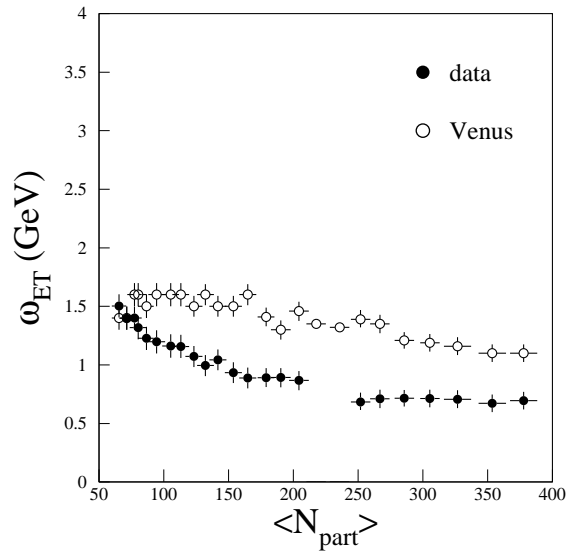


FIG. 16. Centrality dependence of the relative fluctuations in transverse energy,  $E_T$ , with the centrality selected from the  $E_F$ . The result is compared to VENUS using similar centrality selection criteria.